Electronic Supplementary Information (ESI)

to:

Carbon Coated Microshells Containing Nano-Sized Gd(III) Oxidic Phases for Multiple Bio-medical Applications

Aldo Arrais,[a] Mauro Botta,[b] Stefano Avedano,[b] Giovanni Battista Giovenzana,[c] Eliana Gianolio,[d] Enrico Boccaleri,[a] Pier Luigi Stanghellini[a*] and Silvio Aime[d*]

[a]Dipartimento di Scienze e Tecnologie Avanzate e Centro NanoSi.S.Te.M.I., Università degli Studi del Piemonte Orientale "A. Avogadro", Via Vincenzo Bellini 25/G, 15100 Alessandria, Italy. E-mail: pierluigi.stanghellini@mfn.unipmn.it

[b]Dipartimento di Scienze dell'Ambiente e della Vita, Università degli Studi del Piemonte Orientale "A. Avogadro", Via Vincenzo Bellini 25/G, 15100 Alessandria, Italy.

[c c] DiSCAFF & DFB Center, Università degli Studi del Piemonte Orientale "A. Avogadro", Via Giovanni Bovio 6, 28100 Novara, Italy.

[d]Dipartimento di Chimica I.F.M. e Centro di Eccellenza per l'Imaging Molecolare, Università degli Studi di Torino, Via Pietro Giuria 7, 10125 Torino e Via Nizza 52, 10126 Torino, Italy. E-mail: silvio.aime@unito.it

1. Details on the chemical synthesis of the capsular Gd@C material.

Humic acid (HA, **Fig. S1**) is a convenient raw source of carbon, as it contains both aliphatic and aromatic carbon frameworks in different statistical isomeric arrangements. Hence, it provides the ideal starting reactant material for capsules pyrolitic growth process. The aromatic fraction of HA is highly desirable, because it constitutes the pre-formed reactant structure for the final protective graphitisation, obtained after thermal treatment. Besides, HA contains different oxygen groups (*i.e.*, mostly hydroxylic, ketonic and carboxylic units), which are likely to act as efficient sequestering ligands for cationic transition metal ions.
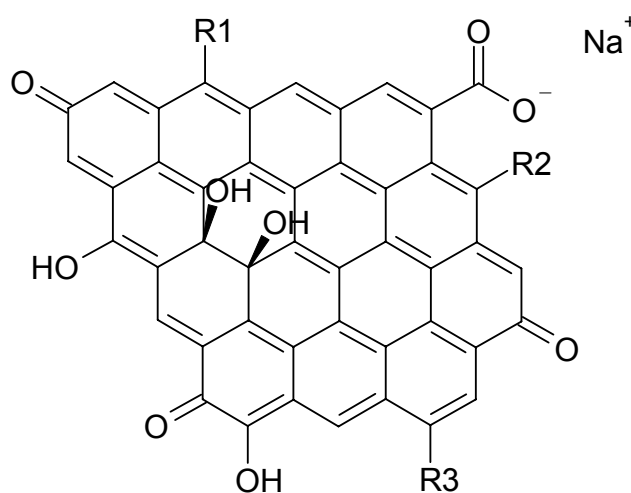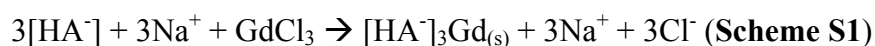

Fig. S1. *A schematic representative model of sodium salt of humic acid (HA). The polycondensed aromatic portion of the structure is evidenced (R1, R2, R3 indicate the different HA aliphatic portions).*

Therein, gadolinium is added as GdCl$_3$ salt to concentrated water solutions of HA sodium salts. A salt metathesis is promptly achieved, determining the immediate precipitation of the complex matter humic acid-gadolinium (hereafter, HA-Gd), according to the general scheme reported below:

$$3[HA^-] + 3Na^+ + GdCl_3 \rightarrow [HA^-]_3Gd_{(s)} + 3Na^+ + 3Cl^- \textbf{ (Scheme S1)}$$

2

After the complete sedimentation of the HA-Gd insoluble material, removal of the surnatant aqueous solution eliminates the NaCl by-product. However, as revealed by the SEM-EDAX analyses, a few residual extent of chlorides, acting as counter-anions to balance the positive charges of the Gd(III) ion, may be occasionally found in the HA-Gd precursor matter. After drying in oven at 65 °C for 1 h, the HA-Gd powders were mechanically milled in an agate mortar and then transferred into alumina vessels, for the further thermal treatment (8 h). Pyrolisis of the HA-Gd precursor (typically, 30-75 mg per treated sample) was performed in a quartz tubular oven (with approximate dimensions of 120 cm length x 7 cm diameter), under strict N_2 anaerobic conditions (under a nitrogen stream $\geq$ 10 mL/min). A final temperature of 1000 °C was reached during the process. A typical complete thermal profile for the HA-Gd precursor is reported in Fig. S2.
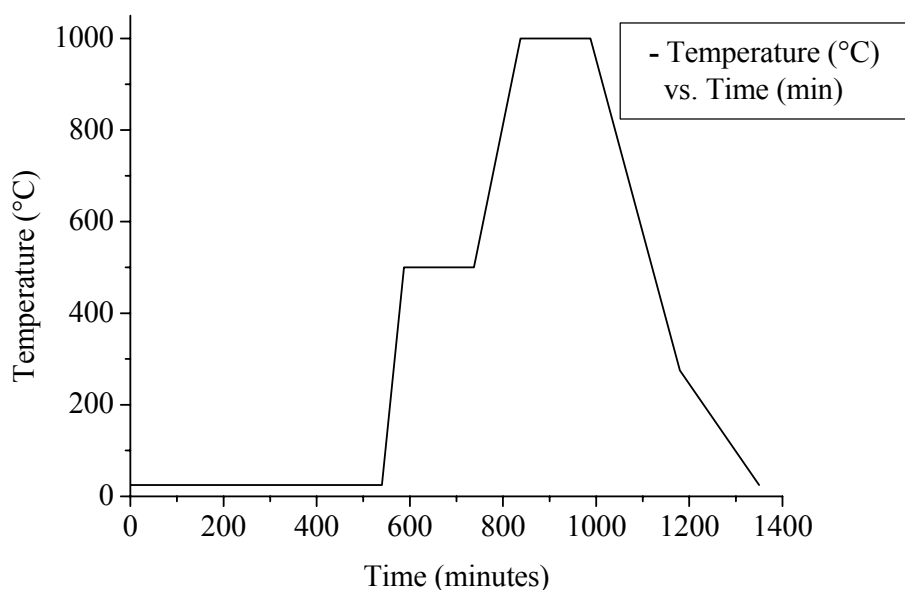

Fig. S2. *An exemplificative complete thermal profile of the pyrolitic treatment of the HA-Gd precursor.*

In the optimised experiment, a first dwell at 500 °C for 2.5 h is required in order to start the graphitisation process of the humic acidic matter and prevent the volatility at high temperature. A further ramp increases the temperature up to 1000 °C, which is then maintained for 2.5 h in order to complete and improve the quality of the external protective coating. During the thermal cooling, air

is allowed to penetrate the tubular oven for T < 275 °C. This promotes a partial aerobic oxidation of the graphitic surfaces of the external carbon coating without damaging the continuous network (cfr. Section 5). The oxidation process inserts polar oxygen groups on the surface of the GdOx@C matter and contributes to increase its hydrophilicity.

2. Hydrophilic sulphonation of the GdOx@C material.

Polar $-SO_3^-$ pendant groups covalently attached on the surface of GdOx@C are inserted by use of the polar zwitterionic sulphonic arene diazonium salt, according to the proposed reported in the following equation:

$$GdOx@C + {}^+N \equiv N\text{-}Ar\text{-}SO_3^-\ (3:2\ THF/H_2O\ mixture) \rightarrow GdOx@C(\text{-}ArSO_3^-)_n(\text{-}OH)_n + nH^+$$

The reaction is performed in a 5 mL glass vial at room temperature by stirring a suspension of GdOx@C (typically, ca. 25-50 mg) with a large excess of the zwitterionic salt (ca. 175-350 mg) for 3 h. The development of the reaction is accompanied by formation of nitrogen bubbles. The reacted material, indicated as GdOx@C-ArSO$_3^-$, is allowed to settle for 12 h and the organic-aqueous solvent mixture, containing the excess of the reactive diazonium salt, is then removed. In order to ensure the complete removal of all reactant traces, GdOx@C-ArSO$_3^-$ is precipitated from an aqueous suspension after neutralization with NaOH.

3. XRPD pattern of the GdOx@C-ArSO$_3^-$ material.

XRPD measurements were performed on a Thermo ARL 'XTRA diffractometer, equipped with a 1.540562 Å Cuk$_{\alpha 1}$ X-ray radiation source. The X-ray generator operated at a voltage of 45 KV and a current of 40 mA. A representative diffraction pattern of the GdOx@C-ArSO$_3^-$ material is reported in Fig. S3.
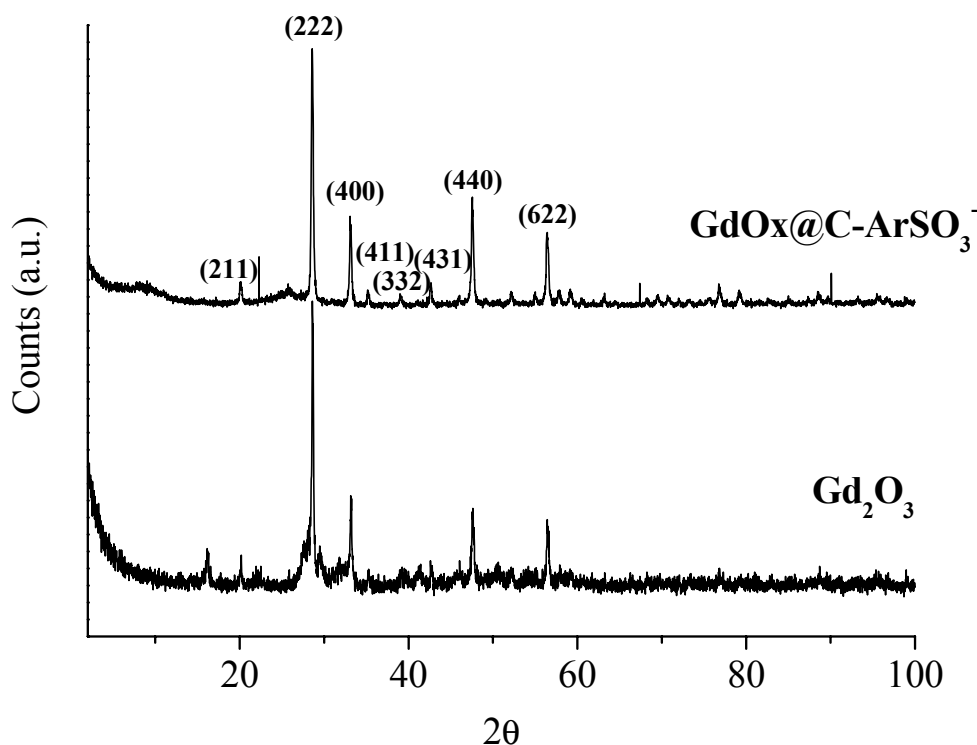
Fig. S3. *XRPD patterns of the GdOx@C-ArSO₃⁻ material (above) and the reference Gd₂O₃ oxide phase (below). The prominent reflections of the cubic Gd₂O₃ structure within the GdOx@C-ArSO₃⁻ material are indexed (ICCD Card no. 12-0797).*

It is evident the formation of an inorganic gadolinium oxide phase which is persistent to the various purification protocols, probably because of the external protecting carbon layers. The weak broad hump at ca. 25 2θ, accompanied by another hampered signal at ca. 8 2θ, is attributable to disordered sp^2 graphitic carbon frameworks of the external coating. As expected from the particularly severe pyrolitic conditions adopted for the capsules formation, even slight modifications of the experimental parameters lead to materials exhibiting variations in the XRPD crystal patterns, although characterised by substantially identical relaxometric properties. In particular, it seems likely that the humidity content of the HA-Gd precursor matter, as well as the residual traces of oxygen present in the tubular oven during the prolonged thermal treatment at 1000 °C can be responsible of the diversity in the inorganic composition of GdOx@C-ArSO₃⁻. In fact, in a few cases we observed the formation of a more complex XRPD pattern that we denote here with II and that is illustrated in Fig. S4.
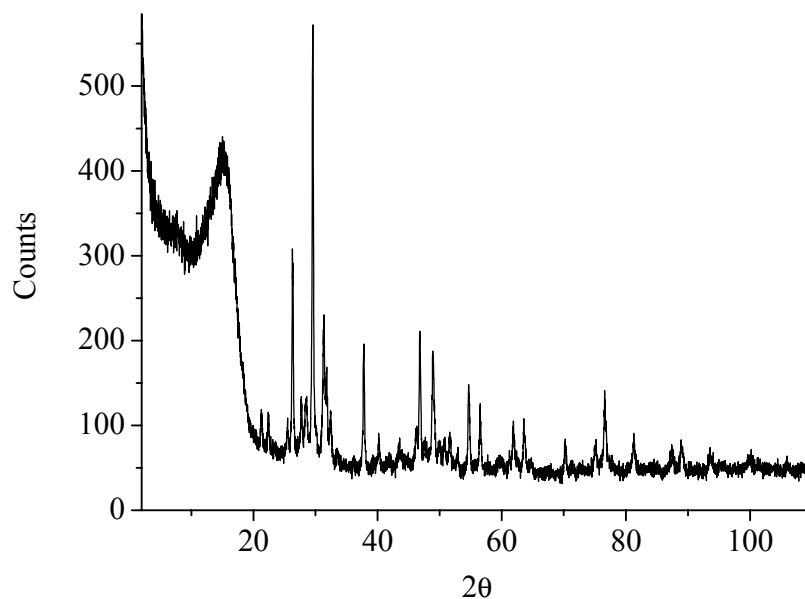
Fig. S4. *XRPD pattern of the GdOx@C-ArSO$_3^-$ (II) material.*

A general inspection of the ICCD database evidences a strict similarity of our GdOx@C-ArSO$_3^-$ (II) inorganic phase with several different Ln$_2$O$_3$ monoclinic structures (Ln = Sm(III), Eu(III), Gd(III), Tb(III); ICCD Cards. nos. 76-0601 and 42-1464, 34-0072, 43-1015, 74-2131). It is important to underline that the relaxometric properties of the aqueous suspensions are not detectably affected by the crystal polymorphism of the Gd(III) oxide.

For all these reasons, it seems rather appropriate the general definition of GdOx@C-ArSO$_3^-$ to indicate the general class of material characterised by substantially coincident morphological and relaxometric properties.

4. Morphological characterisation of the GdOx@C-ArSO$_3^-$ material.

SEM-EDAX analyses were performed on a Leo 450 VP scanning electron microscope. For SEM imaging, the electron probe gun operated normally at a distance of 15 mm from the target, with an electron current of 3.026 A and an accelerating voltage 20 KV. For the EDAX analyses, the

electron probe gun was operating at a distance of 15 mm from the target sample, with electron current typically occurring in the 3-3.5 A, with accelerating voltages in the 15-20 kV range.

TEM analyses were performed on a Philips EM201 transmission electron microscope. Samples of $GdOx@C\text{-}ArSO_3^-$ from dilute aqueous dispersions were evaporated over a measurement grid. The instrument operated at an accelerating voltage of 60 kV, for the acquisition of section images. The selected acquired photographs were finally scanned and digitalised.

From SEM and TEM pictures, a rather wide distribution of the particle sizes is noticed. Contrary to the irregularity of the capsular shapes, that contribute to the enhancement of the transverse relaxivities, the wide size distribution represents an undesirable factor, especially in view of possible *in vivo* MRI applications. In order to optimize the size control different procedures were tested. Filtration of concentrated aqueous dispersions with filters at selected and controlled porosity provided generally scarce results, presumably because of the inactivation of the relatively smaller pores by the largest particles. A more effective size selection was achieved by prolonged sedimentation times. An exemplificative illustration is provided *e.g.* in Fig. S5, where the capsule size distribution of the $GdOx@C\text{-}ArSO_3^-$ material has been calculated after a SEM microscopy observation reported in Fig. S6.
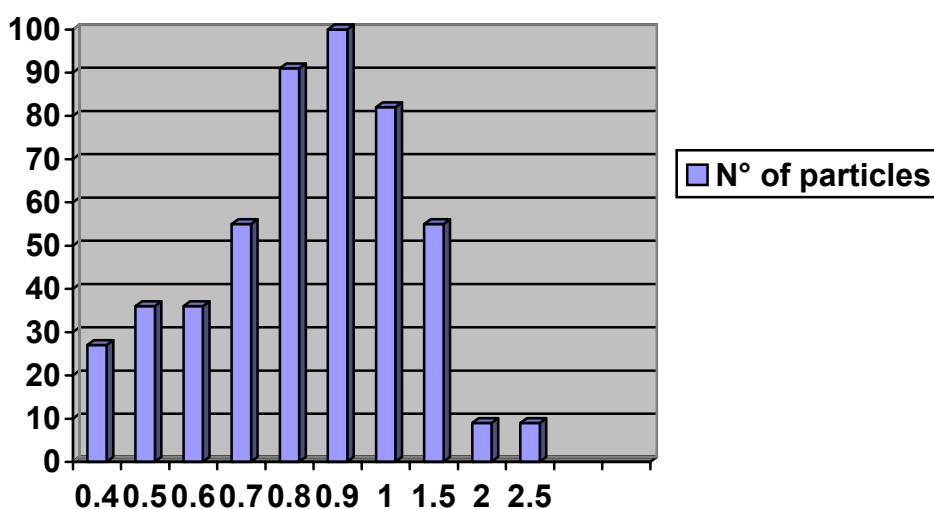

Fig. S5. Normalized relative particle diameter size (μm) distribution of $GdOx@C\text{-}ArSO_3^-$ capsules taken from the SEM image of Fig. S6 (below).

The image was scanned on the aqueous dispersion (2-3 water drops onto the SEM measurement platelet) after 15 min of sedimentation of the hydro-dispersible matter.
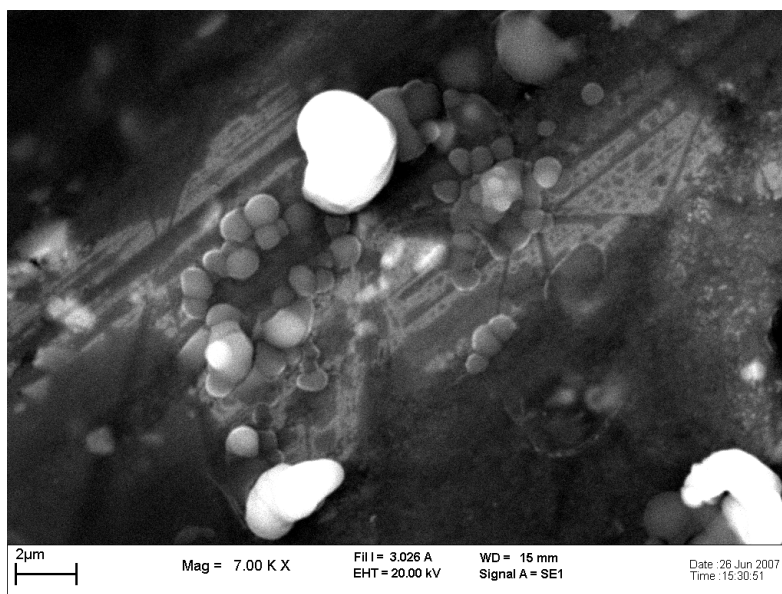

Fig. S6. *SEM image of the GdOx@C-SO$_3^-$ material referred to the capsule size distribution calculated in Fig. S5.*

However, further experimental work is necessary in order to strictly control the dimensional distribution, crucial for the development of diagnostic and therapeutic bio-medical applications.

5. TGA characterisation of the GdOx@C-ArSO$_3^-$ material.

TGA measurements were performed on a Setaram SetSys Evolution TGA/DSC instrument. The GdOx@C-ArSO$_3^-$ samples (5-20 mg) were heated in air atmosphere from 50 to 1200 °C with an heating rate of 10 °C/min using standard 10 μL platinum crucibles. The air gas flow was set at 20 mL/min. A blank response curve using the same conditions was collected and subtracted to remove instrumental and experimental bias effects. The curves were rescaled to weight percent, using the initial mass of the sample. Derivative curves were calculated using the variation of weight

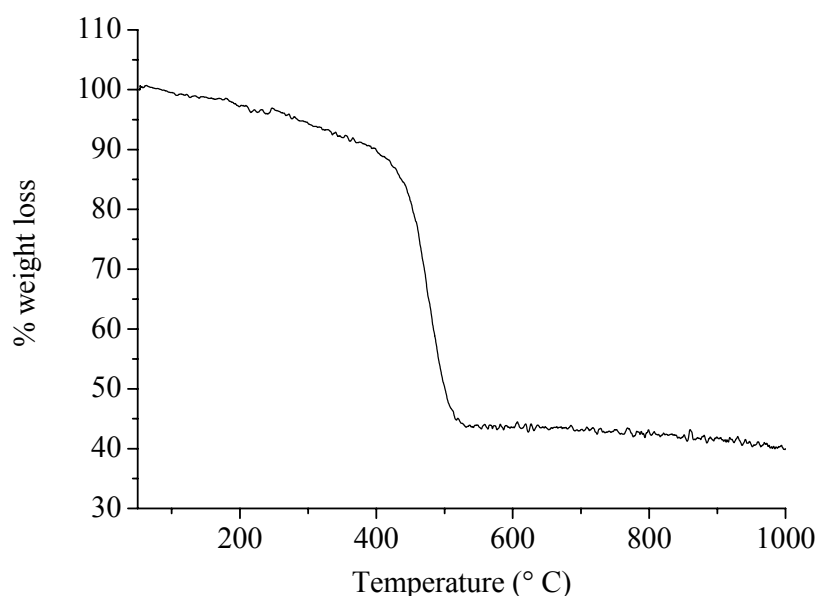over temperature change. A representative TGA profile obtained under aerobic conditions is shown in Fig. S7.

Fig. S7. *TGA profile of the aerobic degradation of GdOx@C-ArSO$_3^-$ material.*

A first, minor weight loss (ca. 10%) below ca. 400 °C is attributed to the degradation of the attached hydrophilic sulphonic appendages. Above 400 °C, a significant weight loss, reducing the starting mass down to ca. 45%, can be related to the aerobic degradation of the protective carbon layers. The observation confirms the thermal stability of this material which results to be air-resistance towards degradation up to ca. 400 °C. Finally, the residual mass, which does not change with progressive temperature increase up to 1000 °C, can be assigned to the inorganic phase.

6. Spectroscopic characterisation of the Gd@C-ArSO$_3^-$ material.

Raman measurements.

Raman spectra were acquired on a Bruker RFS100 spectrophotometer, equipped with a Nd:YAG laser, emitting at 1,064 μm, as the excitation source, and a liquid-nitrogen cooled Ge detector. Employed laser irradiating powers normally occurred in the 50-75 mW range. Instrumental resolution was set at 4 cm^{-1}. According to the optimisation of laser focalisation, 5000-

15000 scansion were typically acquired and averaged. In Fig. S8, the solid-state Raman spectrum of
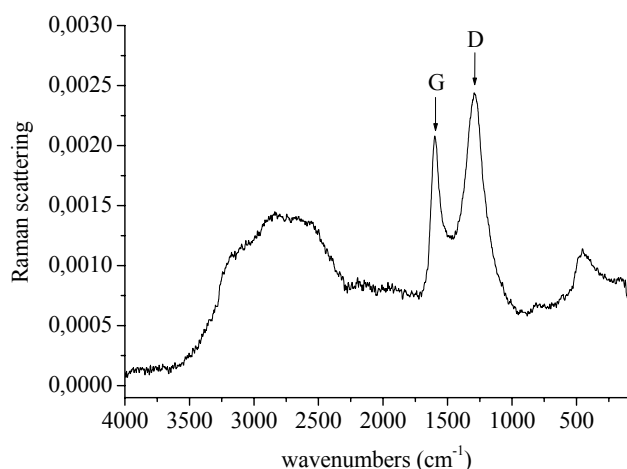
GdOx@C-ArSO$_3^-$ material is reported.

Fig. S8. *Solid state Raman spectrum of GdOx@C-ArSO$_3^-$.*

The emerging presence of the two diagnostic G and D bands of sp^2 carbon graphitised

systems is apparent. The G band (ca. 1600 cm^{-1}) is related to the carbon graphitic skeletal frame and

the D band (ca. 1280 cm^{-1}) reflects the defectivity of the graphitic network. Interestingly, these

diagnostic peaks are observed also in concentrated aqueous dispersions (Fig. S9). In both cases, it is

noteworthy the great Raman intensity of the G and D peaks, probably enhanced by the presence of

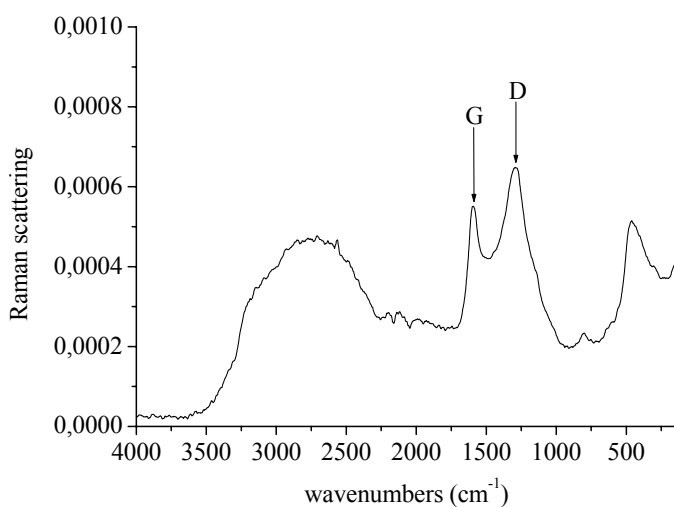the sub-standing Gd lanthanide metal embedded within the inorganic phase.

Fig. S9. *Raman spectrum of water-dispersed GdOx@C-ArSO$_3^-$.*

FT-IR measurements.

FT-IR spectra were recorded on Bruker Equinox 55 spectrophotometer. Samples were milled in an agate mortar and pressed within a KBr hosting matrix. Instrumental resolution was set at 2 cm^{-1}. A representative FT-IR spectrum is shown in Fig. S10. With respect to a blank reference of KBr matrix, the enhanced surface hydrophilicity of the functionalised GdOx@C-ArSO$_3^-$ material is observed. As expected, no significant vibrational information can be extracted on the carbonaceous coating. The structured profile of the broad band set around 1600 cm^{-1} is possibly pertinent to a residual presence of carboxylate groups on the capsular surface. A few observed vibrational absorptions, within the 1230-1040 cm^{-1} zone, might be properly representative of the –SO$_3^-$ sulphonic groups, belonging to the covalently attached appendages. However, the exiguous relative extent of the attached moieties with respect to the bulk of the GdOx@C-ArSO$_3^-$ material lowers severely the spectral intensity of the diagnostic signals for the inserted structures.

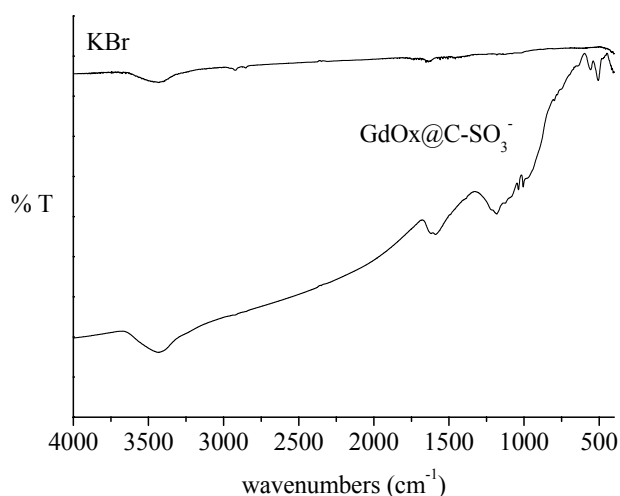**Fig. S10.** *FT-IR spectrum of GdOx@C-ArSO$_3^-$.*

7. Pre-assessment of the absence of free external gadolinium in the GdOx@C-ArSO$_3^-$ material before cellular uptake experiments.

Before the cellular adhesion experiments, the absence of the free Gd(III) cations external to the capsules protective coating was further checked. The gadolinium leakage from the material was

ruled out on the basis of the orange xylenol dye procedure.[1SI] Aqueous suspensions of the material were allowed to slowly precipitate or they were gently centrifuged at acidic pH. In this way, the possible external gadolinium is present as solvated aqua-ion. An aliquot of the surnatant (70 µL) is then added to the standard dye solution (700 µL) and the absorbance of the resulting solution is measured at the diagnostic wavelengths (*i.e.*, 573 and 433 nm). From a calibration line, it was possible to determine an average sub-micromolar amount of Gd(III), hence ensuring the suitability of the GdOx@C-ArSO$_3^-$ material for cell tests (the total Gd(III) shielded concentrations determined by ICP range over the millimolar threshold).

Reference

[1SI]*cfr.* A. Barge; G. Cravotto; E. Gianolio; F. Fedeli. *Contr. Med. Mol. Imag.*, **2006**, *1*, 184-188.